

Kinetics and Structure of Self-Assembled Flagellin Monolayers on Hydrophobic Surfaces in the Presence of Hofmeister Salts: Experimental Measurement of the Protein Interfacial Tension at the Nanometer Scale

Boglarka Kovacs, Andras Saftics, Attila Biro, Sandor Kurunczi, Balazs Szalontai, Balazs Kakasi, Ferenc Vonderviszt, Andras Der, and Robert Horvath

J. Phys. Chem. C, **Just Accepted Manuscript** • DOI: 10.1021/acs.jpcc.8b05026 • Publication Date (Web): 27 Aug 2018

Downloaded from <http://pubs.acs.org> on September 2, 2018

Just Accepted

“Just Accepted” manuscripts have been peer-reviewed and accepted for publication. They are posted online prior to technical editing, formatting for publication and author proofing. The American Chemical Society provides “Just Accepted” as a service to the research community to expedite the dissemination of scientific material as soon as possible after acceptance. “Just Accepted” manuscripts appear in full in PDF format accompanied by an HTML abstract. “Just Accepted” manuscripts have been fully peer reviewed, but should not be considered the official version of record. They are citable by the Digital Object Identifier (DOI®). “Just Accepted” is an optional service offered to authors. Therefore, the “Just Accepted” Web site may not include all articles that will be published in the journal. After a manuscript is technically edited and formatted, it will be removed from the “Just Accepted” Web site and published as an ASAP article. Note that technical editing may introduce minor changes to the manuscript text and/or graphics which could affect content, and all legal disclaimers and ethical guidelines that apply to the journal pertain. ACS cannot be held responsible for errors or consequences arising from the use of information contained in these “Just Accepted” manuscripts.



1
2
3 **Kinetics and Structure of Self-assembled Flagellin Monolayers on**
4 **Hydrophobic Surfaces in the Presence of Hofmeister Salts:**
5 **Experimental Measurement of the Protein Interfacial Tension at**
6 **the Nanometer Scale**
7
8
9

10 Boglarka Kovacs^{1,2}, Andras Saftics¹, Attila Biro¹, Sandor Kurunczi¹, Balazs Szalontai³,
11 Balazs Kakasi⁴, Ferenc Vonderviszt^{1,4}, Andras Der³ and Robert Horvath^{1,2*}
12

13 ¹*Nanobiosensorics Group, Institute of Technical Physics and Materials Science, Centre for*
14 *Energy Research, Konkoly-Thege út 29-33, Budapest, Hungary*
15

16 ²*Chemical Engineering and Material Science Doctoral School, University of Pannonia,*
17 *Egyetem u.10, Veszprém, Hungary*
18

19 ³*Biomolecular Electronics Research Group, Bio-nanoscience Research Unit, Institute of*
20 *Biophysics, Biological Research Centre, Hungarian Academy of Sciences, Temesvári krt. 62.,*
21 *Szeged, Hungary*
22

23 ⁴*Bio-Nanosystems Laboratory, Research Institute of Biomolecular and Chemical*
24 *Engineering, University of Pannonia, Egyetem u. 10, Veszprém, Hungary*
25
26
27
28

29 *Corresponding author
30

31 Email: horvath.robert@energia.mta.hu, Phone: 003613922696
32
33
34
35
36
37
38
39
40
41
42
43
44
45
46
47
48
49
50
51
52
53
54
55
56
57
58
59
60

Abstract

In the present study, we monitor the adsorption-desorption kinetics and adsorbed layer structure of the bacterial protein flagellin in the presence of Hofmeister salts by a surface sensitive label-free optical biosensor (optical waveguide lightmode spectroscopy, OWLS). The recorded OWLS data were analyzed by a computer code using a set of coupled differential equations modeling the adsorption-desorption process. By supposing reversibly and irreversibly adsorbed protein states with different adsorption footprints, the kinetic data could be perfectly fitted. We revealed that the proteins adsorbing in the presence of kosmotropic salts had smaller footprints, leading to a more oriented and densely packed layer. Kosmotropic salts increased both the adsorption rate constant and the transition rate constants from the reversibly to the irreversibly adsorbed state. In contrast, chaotropic salts increased the desorption rate constant and led to decreased adsorbed mass and a more loosely packed film. Neither circular dichroism spectroscopy in bulk solutions or Fourier transform infrared spectroscopy of surface-adsorbed flagellins could reveal significant structural changes due to the presence of the Hofmeister salts, and supported our conclusions about the adsorption mechanism. Based on the measured kinetic and structural data (footprints of adsorbed proteins), we developed a model to calculate the protein-water-substrate interfacial tension in the presence of Hofmeister salts, and compared the experimentally obtained values with related literature data. The calculated values are consistent with previously published data of surface tension changes, and - to the best of our knowledge - represent the first experimental results for this quantity.

1. Introduction

The proper control of interfaces between artificial devices and biomaterials is a key issue in modern biological and medical sciences. Biofunctionalized surfaces, that play a vital role in various biosensor and drug delivery applications, are expected to provide high specificity toward the target molecules, and at the same time should not show any non-specific binding. In view of these challenging requirements, we have recently suggested and accomplished a procedure for coating of solid surfaces by flagellin molecules. Flagellins are the building blocks of bacterial flagellar filaments. The filament is composed of thousands of flagellin subunits. Flagellin consists of 4 domains: D0, D1, D2, and D3. Both terminal regions of the molecule (forming D0 and partly D1) are disordered in the monomeric form¹. These regions are rich in hydrophobic amino acids and play an important role for effective and fast self-assembly by hydrophobic interactions to form flagellar filaments¹. Polymerization of flagellin is accompanied by an ordering of the terminal regions into α -helical bundles in the inner core of the filaments. Note, these disordered regions are expected to easily adapt to the local environment. As we have shown, flagellin does not preferentially adsorb on hydrophilic substrates, but very rapidly forms an oriented, dense and stable monolayer on hydrophobic surfaces, where the hypervariable D3 domain is oriented towards the solution^{2,3}. It presents a repellent surface coating to bacteria or cancer cells^{3,4}. Moreover, appropriate modifications of the D3 domain by genetic engineering can also be used to fabricate specific recognition sites for a wide range of targeted analytes^{3,5-7}.

For practical applications, the orientation of flagellin molecules and their surface coverage should be maximized and well-controlled. To this end, understanding the main factors determining the interactions of flagellin domains with surfaces is of pivotal importance. Since the formation of the flagellin layer takes place in a complex, aqueous environment, hydrophobic interactions are assumed to play a dominant role. (Note that we use the term „hydrophobic interaction” in a very general sense, namely, by quantifying it with the change of the interfacial term of the Gibbs free energy by unitary surface change taken place upon the interaction: $\Delta G/\Delta A$, i.e., a sort of interfacial tension: γ , assuming that the hydrophobic effect is proportional to the solvent-exposed surface area⁸⁻¹⁰.) On the other hand, “kosmotropic” (water-structure making) and “chaotropic” (water-structure breaking) co-solutes (neutral salts) are known to modify protein interactions, called Hofmeister effects^{11,12}, via affecting the interfacial tension of macromolecules^{13,14}. A plethora of experimental studies proves that such “Hofmeister salts” can affect protein structure, function, and aggregation¹⁵⁻²⁰. It was

1
2
3 shown that kosmotropic anions (F^- , CH_3COO^- , SO_4^{2-} , etc.) increase, while chaotropic ones
4 (Br^- , I^- , SCN^- , ClO_4^- , etc.) decrease the effective protein-water interfacial tension (γ)^{14,21}.
5
6 Earlier studies indicate that these ions influence the adsorption process of globular proteins to
7 solid surfaces as well^{22,23}. Hofmeister effects on the film-forming properties of such a
8 complex, anisotropic and amphiphilic protein as flagellin, however, have not been
9 investigated in detail, yet.
10
11

12
13 In this paper, we have studied how Hofmeister salts affect the morphological properties of
14 thin flagellin films, and provide indirect evidence that flagellin adsorption to a hydrophobic
15 surface is mainly governed by hydrophobic effects” (i.e., by surface terms of the Gibbs free
16 energy). To monitor the adsorption process optical waveguide lightmode spectroscopy
17 (OWLS) was used. OWLS utilizes two modes of the light passing in the waveguide: the
18 transversal electric (TE) and magnetic (TM) modes which provide information not only about
19 the amount but on the anisotropy of the adsorbed layer as well. OWLS is also perfectly suited
20 to analyze adsorption-desorption processes with high resolution^{24–26}. We show that
21 kosmotropic salts increase flagellin packing density and molecular orientation, while
22 chaotropic ions act in the opposite direction. To analyze the data and to determine the key
23 parameters of the adsorption-desorption process, we set up two kinetic models (a parallel and
24 a consecutive) based on a series of coupled differential equations. Importantly, not only the
25 rate constants of the adsorption-desorption processes were fitted, but our model allowed to
26 determine the footprints of the adsorbed proteins at the nanometer scale. Circular dichroism
27 spectroscopy (CD) and Fourier transform infrared experiments in attenuated total reflection
28 mode (FTIR-ATR) have been used to detect conformational changes of flagellins upon
29 adsorption to solid surfaces under the effect of the presence of characteristic Hofmeister salts.
30
31

32
33 Based on the fitted kinetic rate constants of the processes and the adsorbed molecular
34 footprints, we set up a model to first experimentally derive a quantitative value of the protein
35 interfacial tension (PIT). PITs are useful parameters to interpret Hofmeister phenomena, such
36 as, e.g., cosolute-induced changes of aggregation and conformational states, or related
37 alteration in protein function, where protein-water interfacial tension (γ_{pw}) can be considered
38 as the main driving force of the effects^{13,14}.
39
40

41
42 Analogously, the interaction of proteins with various substrates, which can either be
43 molecular ones (such as cofactors, lipids, nucleic acids and other proteins) or macroscopic
44 solid surfaces (like in the case of adsorption processes) are expected to be understood on the
45
46
47
48
49
50
51

1
2
3 phenomenological level using a more complex PIT, the protein-water-substrate interfacial
4 tension (γ_{pws}). We define this quantity as the specific work of adhesion, i.e., $\gamma_{pws} = \Delta G/\Delta A$,
5 where ΔG and ΔA stand for molecular changes of the Gibbs free energy accompanying the
6 interactions and water-exposed surface area change upon the protein adsorption process,
7 respectively. Since γ_{pws} , alike surface tensions in general, represents an interfacial energy
8 density, we call it, hereafter, interfacial tension. Note that while in protein aggregation the
9 pairwise interacting surfaces are considered to be identical (and ΔG is called cohesion
10 energy), during surface adsorption they are usually different. Nonetheless, γ_{pw} can be
11 considered as a special case of the generalized PIT, γ_{pws} , which quantifies the strength of the
12 hydrophobic interaction between protein and substrate. It should depend on the
13 hydrophobic/hydrophilic properties of both the substrate and the protein, as well as on the H-
14 bonding properties of water itself, which are modulated by the Hofmeister salts. As we show
15 later in this work, $\gamma_{pws} = (\gamma_{pw} + \gamma_{sw} - \gamma_{ps})$, where indices refer to the phases (p: protein, w:
16 aqueous solution, s: substrate) involved in the pairwise interfacial tensions, respectively.
17
18
19
20
21
22
23
24
25

26 We determined γ_{pws} values to characterize the interaction of flagellins with a silanized surface
27 in various kosmotropic and chaotropic salt solutions, giving a simple clue to interpret the
28 protein adsorption process.
29
30

31 In addition to their significance in applied biosensors, the results are expected to have
32 important implications in basic surface science, as well, by revealing some aspects of the
33 adsorption kinetic and protein dynamic processes taking place at complex bio-interfaces.
34
35
36
37
38
39
40
41
42
43
44
45
46
47
48
49
50
51
52
53
54
55
56
57
58
59
60

2. Materials and Methods

2.1. Employed Hofmeister solutions

We applied different salts to influence the protein adsorption: Na_2SO_4 , NaF, CH_3COONa (hereafter NaOAc) (kosmotropic), NaCl (neutral), NaBr, NaI, NaClO_4 (chaotropic), respectively. During the experiments Hofmeister salt concentrations were 720 mM in the presence of 1x PBS at pH 7.4.

2.2. Surface modification

The surface modification of the sol-gel SiO_2 - TiO_2 planar optical waveguides (MicroVacuum Ltd., Hungary) started with a standard cleaning protocol: the chips were soaked for 3 min in chromosulfuric acid (VWR International), rinsed in Milli-Q ultrapure water, immersed into 1 M KOH solution, and then rinsed in copious amounts of ultrapure water. This procedure yielded hydrophilic surface.

The hydrophobicity of surfaces was increased with hexamethyldisilazane (HMDS, Alfa Aesar) treatment using xylene reflux. The employed protocol resulted in water contact angles of 90 – 95° ².

2.3. Contact angle measurement

Water contact angle measurements were carried out at room temperature. Water drops of ~ 5 μl were deposited on the surface and left to be stabilize in a closed chamber saturated with water vapor before the image was taken. The DropSnake method was used to calculate the contact angle²⁷.

2.4. Flagellin preparation and solutions

Filament samples from *Salmonella* cells were prepared as described earlier²⁸. Purified filaments were dissolved in 10 mM PBS at 5 mg/ml concentration. Heat treatment (15 min incubation at 70°C) of the filament induces depolymerization and results in monomeric flagellin units. The solution was centrifuged through a 100 kDa filter (Millipore, UFC510008) to remove aggregates or fragments of filaments still remaining in the sample. Flagellin was diluted with the appropriate 900 mM salt solution (limited by the solubility of NaF) to a final concentration of 1 mg/mL in 720 mM salt.

2.5. Optical waveguide lightmode spectroscopy (OWLS)

We applied the OWLS 210 (MicroVacuum Ltd., Hungary) temperature controlled instrument to monitor the surface adsorption of the proteins. The sensing principle of OWLS is based on the evanescent waves of the guided light. The evanescent field extends a few hundred nanometers above the waveguide surface with a penetration depth of around 100 nm. This is used to probe the change in local refractive index in the proximity of the sensor surface²⁹. Recording the effective refractive index values (N_{TE} , N_{TM}) during the adsorption of protein molecules onto the waveguide surface, the refractive index (n_A) and the thickness (d_A) of the adsorbed layer can be simultaneously determined. The surface mass density (M) can be calculated using the calculated n_A and d_A data and the de Feijter's formula³⁰

$$M = d_A \frac{n_A - n_C}{\frac{dn}{dc}} \quad (1)$$

where n_C is the refractive index of the cover medium, dn/dc is the refractive index increment of the buffer medium containing the adsorbing molecules (usually $0.18 \text{ cm}^3/\text{g}$ is used for protein adsorption studies).

The experiments were carried out at $25 \text{ }^\circ\text{C}$ on previously silanized sensor chips. Both the buffer and sample solutions were injected into the flow-through cuvette using an Ismatec Reglo Digital peristaltic pump having 8 rollers at a constant flow rate of $1 \text{ } \mu\text{l/s}$. After obtaining a stable buffer baseline, the flagellin solution was introduced into the cuvette for 30 min which was followed by another 30 min buffer wash. All experiments were repeated at least three times.

2.6. The basics of the kinetic modeling

In order to model the flagellin adsorption and desorption, the following two models were tested. We have developed a MATLAB code to fit the equations. These models were originally developed by Ramsden and co-workers³¹⁻³³. The consecutive model supposes a reversibly adsorbed molecular state which can desorb or transform to an irreversibly adsorbed state. In contrast, no surface transformations are supposed in the parallel model, the molecules can readily adsorb from solution to an irreversible or a reversible molecular state.

Parallel model

In case of the parallel model the net rates of the protein adsorption of the reversible and irreversible forms are the following:

$$\frac{dM_r}{dt} = k_a c_v \Phi - k_d M_r \quad (2)$$

$$\frac{dM_i}{dt} = k_i c_v \Phi \quad (3)$$

We suppose that the protein can adopt two types of adsorbed states on the surface. The first state refers to reversibly adsorbed molecule with a total protein mass of M_r . The other state is that of the irreversibly adsorbed molecules, having a total mass of M_i . Molecules from the close vicinity of the surface adsorb reversibly with a kinetic rate constant of k_a . The reversibly adsorbed molecules can leave the surface back to the bulk with a desorption rate constant of k_d . The molecules adsorb irreversibly to the surface with a kinetic rate constant of k_i . In the following expressions, c_v denotes the protein concentration in the diffusion boundary layer, Φ is the so-called available area function, which was obtained from numerical simulations³¹

$$\Phi = \frac{(1 - \theta)^3}{1 - 0.812 \cdot \theta + 0.2336 \cdot \theta^2 + 0.0845 \cdot \theta^3} \quad (4)$$

$$\theta = \frac{1}{\Theta_\infty} \left(\frac{M_r}{m/a_r} + \frac{M_i}{m/a_i} \right) \quad (5)$$

Here, θ is the fraction of total area occupied by adsorbed protein, Θ_∞ is the saturation coverage ($\Theta_\infty = 0.58$ from numerical simulations for molecules with spherocylindric footprint³⁴), m is the mass of a single protein, a_i and a_r are the footprints of the reversibly and irreversibly adsorbed molecules, respectively. The concentration above the adsorbing interface (c_v) is calculated from the following differential equation^{24,35}:

$$\frac{dc_v}{dt} = \frac{1}{\delta} \left(D \frac{c_{\text{bulk}} - c_v}{\delta} + k_d M_r - (k_a + k_i) c_v \Phi \right) \quad (6)$$

where δ is the thickness of the diffusion boundary layer, D is the diffusion coefficient of the protein ($D = 0.74 \text{ cm}^2/\text{s}$ for flagellin), c_{bulk} is the concentration of the injected protein solution.

The thickness of the diffusion boundary layer is calculated using the following expression²⁴:

$$\delta = \left(\frac{3}{2} \right)^{2/3} \left(\frac{D \cdot C}{v_0} \right)^{1/3} \quad (7)$$

where C is the factor determined by the size of the tube ($C = 14.753 \text{ mm}^4$ calculated based on the cuvette geometry), and v_0 is the flow rate of the solution ($v_0 = 1 \text{ } \mu\text{l/s}$).

During the fitting of the above differential equations the free parameters were the following: k_a , k_d , k_i , a_i , and a_r .

Consecutive model

In case of the consecutive model, the net rates of the adsorption corresponding both to the reversible and irreversible forms are the following^{32,33}:

$$\frac{dM_r}{dt} = k_a c_v \Phi - k_d M_r - k_i M_r \quad (8)$$

$$\frac{dM_i}{dt} = k_i M_r \quad (9)$$

Molecules from the close vicinity of the surface adsorb with a kinetic rate constant of k_a . The reversibly adsorbed molecules can either leave the surface moving back to the bulk with a desorption rate constant of k_d or can transform to irreversibly adsorbed state with a rate constant of k_i .

The concentration above the adsorbing interface is calculated from the following differential equation:

$$\frac{dc_v}{dt} = \frac{1}{\delta} \left(D \frac{c_{\text{bulk}} - c_v}{\delta} + k_d M_r - k_a c_v \Phi \right) \quad (10)$$

2.7 Circular dichroism spectroscopy

Far-UV CD spectra were recorded at room temperature in the range of 200-260 nm using standard procedures. The measurements were performed in 1 mm cylindrical quartz cells with a Jasco J-720 spectropolarimeter. Flagellin samples were measured at 0.5 mg/ml protein concentration.

2.8. Fourier transform infrared spectroscopy

Fourier transform infrared spectra were recorded with a Bruker Wertex70 spectrometer equipped with a Platinum Diamond single-reflection ATR unit. Infrared spectra were calculated from 128 co-added interferograms of 2 cm^{-1} spectral resolution, detected by a liquid nitrogen-cooled MCT detector.

1
2
3 The infrared spectra of the adsorbed flagellin were obtained from samples prepared as
4 follows: a droplet (3-5 μl) of the protein solution was placed onto the silanized (hydrophobic)
5 surface, which was left for 3 min in order to deposit the flagellin layer, and then the bulk of
6 the droplet was withdrawn by a pipette. The remaining spot of the droplet was washed twice
7 with 20 μl solution of the respective salt, in between, and at the end the excess volume was
8 withdrawn by a pipette. The wet surface of the flagellin spot was then pressed against the
9 diamond, and its single beam spectrum was taken. Here, care has to be taken of rather quick
10 work because the very small volume of the D_2O of the sample is quickly adsorbing water
11 from air. Within a few minutes before the complete drying, not only HOD bands, but the H_2O
12 deformation band at around 1642 cm^{-1} can appear, thus spoiling the protein structure
13 determination. Therefore, in the presented experiments the washed sample was immediately
14 placed onto the diamond crystal. Once on the crystal, we could not observe H_2O
15 contamination in the samples.
16
17
18
19
20
21
22
23

24 Prior to each sample measurement, the diamond crystal was thoroughly cleaned with water
25 and chloroform, and a reference single beam spectrum was recorded (the cleanness of the
26 diamond was checked by comparing the consecutive reference spectra). The absorption
27 spectra shown in the paper were calculated from the single beam diamond and sample spectra
28 taken them as background and foreground, respectively.
29
30
31

32 For spectrum analysis, the amide I-II regions ($1800\text{-}1500\text{ cm}^{-1}$) were cut out; a linear baseline
33 was fitted to the endpoints of the region and then subtracted. Afterwards the spectra were
34 normalized and fitted with Gaussian component bands. All post-record spectral manipulations
35 were performed with the SPSERV[®] (Cs. Bagyinka, BRC, Szeged).
36
37
38
39
40
41
42
43
44
45
46
47
48
49
50
51
52
53
54
55
56
57
58
59
60

3. Results and Discussion

3.1. Surface adsorption of flagellin monitored by OWLS: surface adsorbed mass densities

First, the optogeometrical parameters of the formed flagellin layers were calculated in time based on the recorded OWLS data. Note, the refractive index of the adlayer is increased from kosmotropic to chaotropic salt (see details later). Next, surface mass densities (as described in Eq. 1) were determined for flagellin adsorbed in the presence of different Hofmeister salts (**Fig. 1**). As a reference, the adsorption in the presence of the Hofmeister-neutral NaCl was also considered. It was found that the kosmotropic Na_2SO_4 , NaF and NaOAc salts increased the surface mass densities. In contrast, the chaotropic NaI, NaClO_4 and NaBr salts decreased the surface mass densities (see **Fig. 1**).

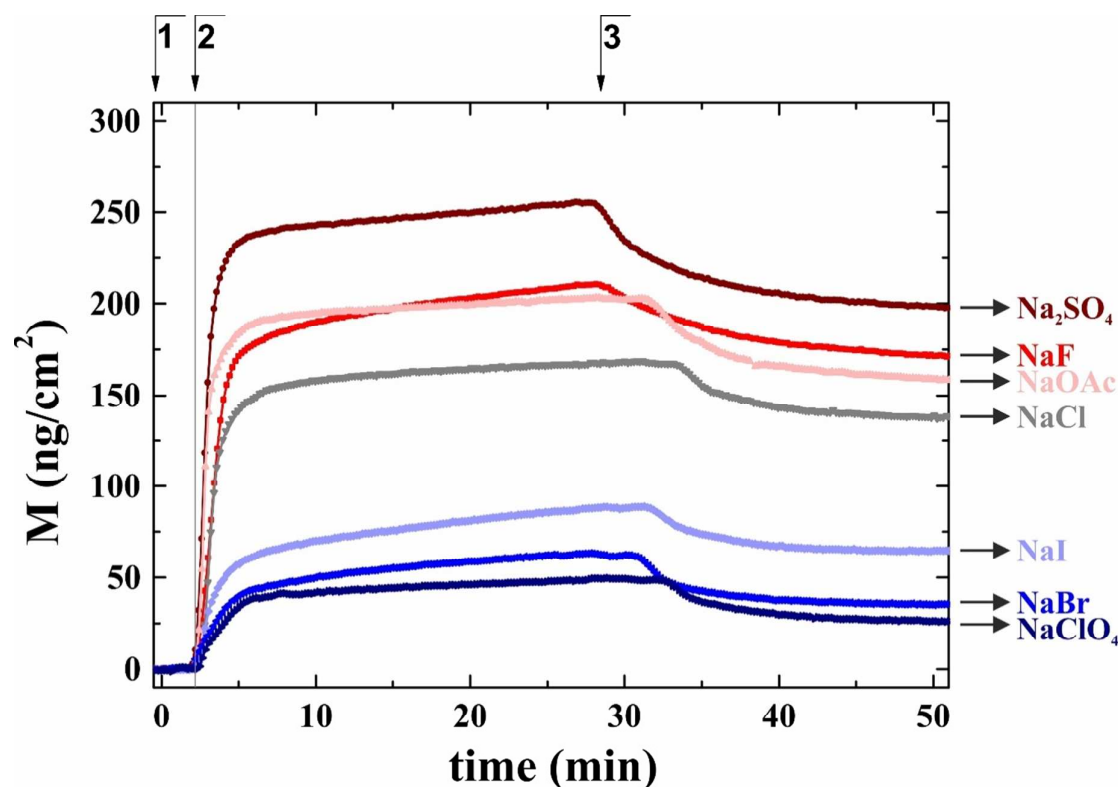


Figure 1 Representative curves of the adsorbed protein surface mass densities in the presence of Hofmeister salts. The kosmotropic salts (*red toned*) increased the surface mass, while chaotropic salts (*blue toned*) decreased the surface mass compared to the Hofmeister-neutral NaCl salt (*grey*). The numbers on the top indicate the following experimental phases: 1: buffer for recording the baseline, 2: injection of flagellin solution, 3: washing with buffer.

The effect of the salts is even more evident in **Fig. 2** where the surface adsorbed masses at the adsorption plateau (just before the washing, M_{plateau}) and at the end of the washing phase (M_{remained}) are plotted. Compared to the NaCl data, the kosmotropes increased the surface mass densities, while the chaotropes decreased them.

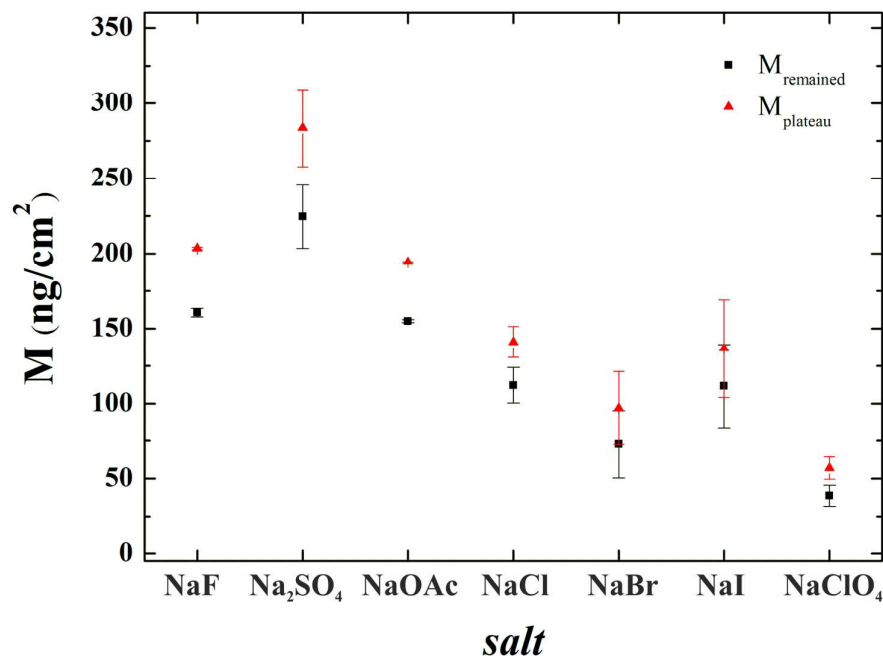


Figure 2 M_{remained} and M_{plateau} values (extracted from the adsorption curves shown in **Fig. 1**) for the different salts studied. Note, that Hofmeister effect is clearly visible both in the plateau and the remaining values of the adsorbed flagellin masses. Both are decreasing in tendency when moving from the kosmotropic salts toward the chaotropic ones.

3.2. The effect of Hofmeister salts on the internal structure of dissolved and surface adsorbed flagellin

CD and FTIR studies were performed to see the effect of Hofmeister salts on the structure of flagellin in solution, and to reveal possible conformational changes upon adsorption onto hydrophobic surfaces. The CD spectra recorded in the presence of various Hofmeister salts were very similar (**Fig. 3a**) indicating that the salts applied had no significant effect on the structure of flagellin in solution. The measured spectra are virtually identical to the CD spectrum of flagellin reported earlier³⁶, and they are characteristic of a protein containing a significant amount of α -helical secondary structure. The D1 domain of flagellin is known to be largely α -helical while the D2-D3 domains are dominated by β -strands¹. The D0 domain, composed of the N- and C-terminal regions of the molecule, has no folded structure in solution but its unstable helical segments also contribute to the observed CD signal³⁶.

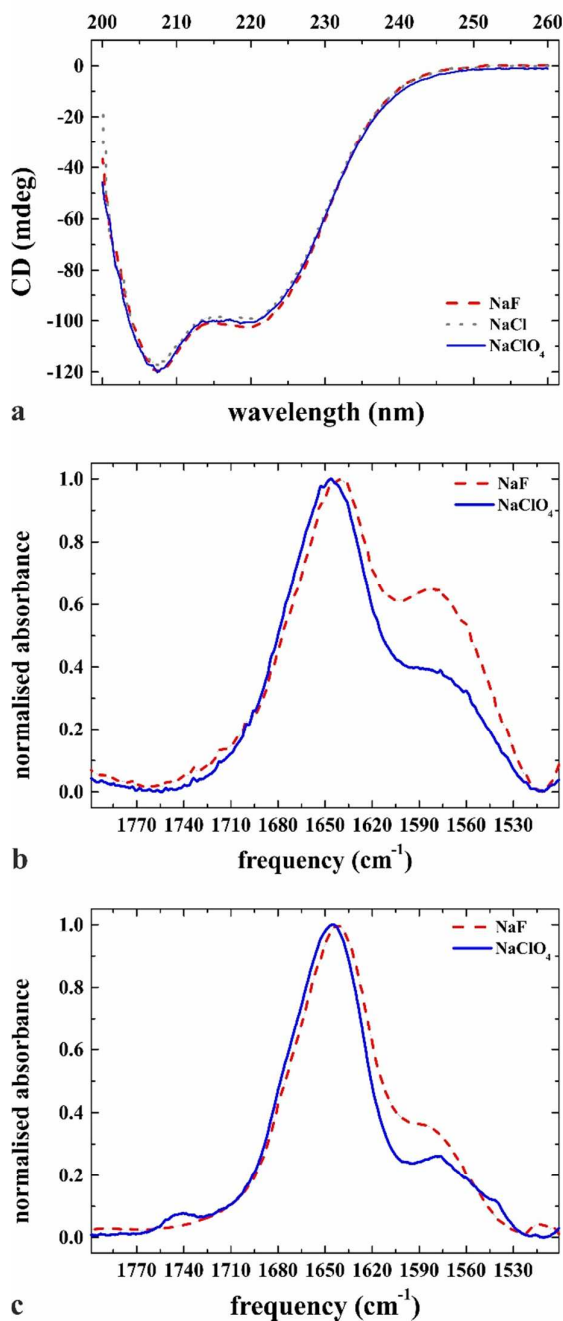


Figure 3 (a) The effect of the Hofmeister salts in solution on the flagellin structure measured by CD spectroscopy. The measurements were done in 10 mM PBS (pH 7.4) containing the kosmotropic NaF (*red*), the neutral NaCl (*grey*) or the chaotropic NaClO₄ (*blue*) at 720 mM concentration. (b) Fourier transform infrared spectra of the Amide I regions of flagellin in bulk solution measured over a diamond crystal in the presence of kosmotropic (NaF, *blue*) and chaotropic (NaClO₄, *red*) Hofmeister salts; (c) after adsorption onto a silanized glass surface in the presence of the same Hofmeister salt-containing solutions.

1
2
3 FTIR spectroscopy was used to study conformational changes related to the surface
4 adsorption of flagellin. As a reference, infrared spectra were first recorded in solution in the
5 presence of the highly kosmotropic and chaotropic NaF and NaClO₄, respectively above the
6 diamond surface of the ATR cell (**Fig. 3b**). For both salts, the Amide I region exhibited a
7 dominant peak at around 1650 cm⁻¹, what is slightly shifted toward lower frequency in the
8 presence of the kosmotropic NaF suggesting subtle conformational rearrangements
9 presumably in the highly flexible terminal regions of flagellin. The component at around
10 1580 cm⁻¹ is assigned to the combination band of D₂O (ν₂ + vibration). Flagellin samples were
11 prepared by heat-induced depolymerization of filament samples dissolved in D₂O containing
12 buffers, but the extent of the H-D exchange was not controlled in our experiments. **Fig. 3c**
13 presents FTIR spectra of flagellin obtained after adsorption onto the hydrophobic surface in
14 the presence of NaF or NaClO₄. The close similarity of the spectra in **Fig. 3b** and **c** in the
15 Amid I region demonstrates that adsorption of flagellin onto the hydrophobic surface did not
16 cause significant structural change of the molecule.
17
18
19
20
21
22
23
24
25

26 Our CD and FTIR experiments demonstrated that the solution structure of flagellin was not
27 significantly influenced by the kosmotropic or chaotropic salts. Our previous study revealed
28 that adsorption of flagellin to a hydrophobic surface in PBS was mediated by the disordered
29 terminal regions of the molecule ². These regions assemble into amphipathic helical bundles
30 upon polymerization, and hydrophobic interactions between these helical bundles govern
31 subunit interactions within the filament core ¹. Our preliminary expectation was that the
32 terminal regions of flagellin are also stabilized into an α-helical conformation when they
33 interact with a hydrophobic surface. However, our FTIR results clearly showed that this was
34 not the case. Helical structures are known to contribute to the FTIR signal mainly in the 1648-
35 1654 cm⁻¹ region while random protein structures give a contribution around 1643 cm⁻¹ ³⁷.
36 Therefore, helical stabilization of the terminal regions should result in a spectral shift towards
37 higher wavenumbers. On the contrary, in the presence of the highly kosmotropic NaF which
38 is expected to strengthen hydrophobic interactions, we observed the opposite effect. It seems
39 that NaF promotes the attachment of flagellin to the silanized surface by inducing subtle
40 rearrangements in the terminal regions which lead to the maximization of the hydrophobic
41 contacts with the silanized glass surface.
42
43
44
45
46
47
48
49
50
51
52
53
54
55
56
57
58
59
60

3.3. Rate constants and adsorbed molecular footprints obtained from the kinetic modeling

Fig. 4a shows the typical concentration profile in the bulk and in the diffusion boundary layer analyzed using the parallel model. Note that the consecutive model gives the same results (data are not shown). The results of the kinetic model fits are shown in **Fig. 4b** and **c** for two typical adsorption-desorption curves. **Fig. 4b** represents the effect of the kosmotropic salt, NaF. NaF increased the measured irreversibly adsorbed protein surface mass density to 168 ng/cm². It was found that a significant proportion of the adsorbed protein binds irreversibly to the hydrophobic surface. The kinetics of flagellin adsorption in the presence of the chaotropic NaClO₄ is shown in **Fig. 4c**. Here, the irreversibly adsorbed flagellin mass reached only a value of 50 ng/cm², which is 3.4 times less than in case of the kosmotropic NaF.

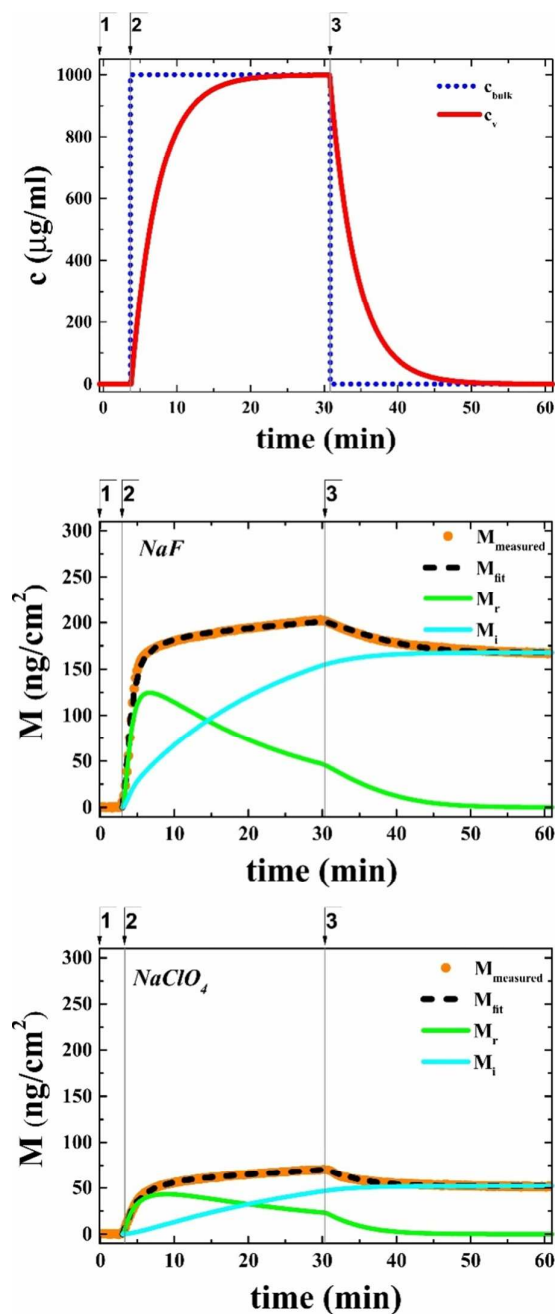
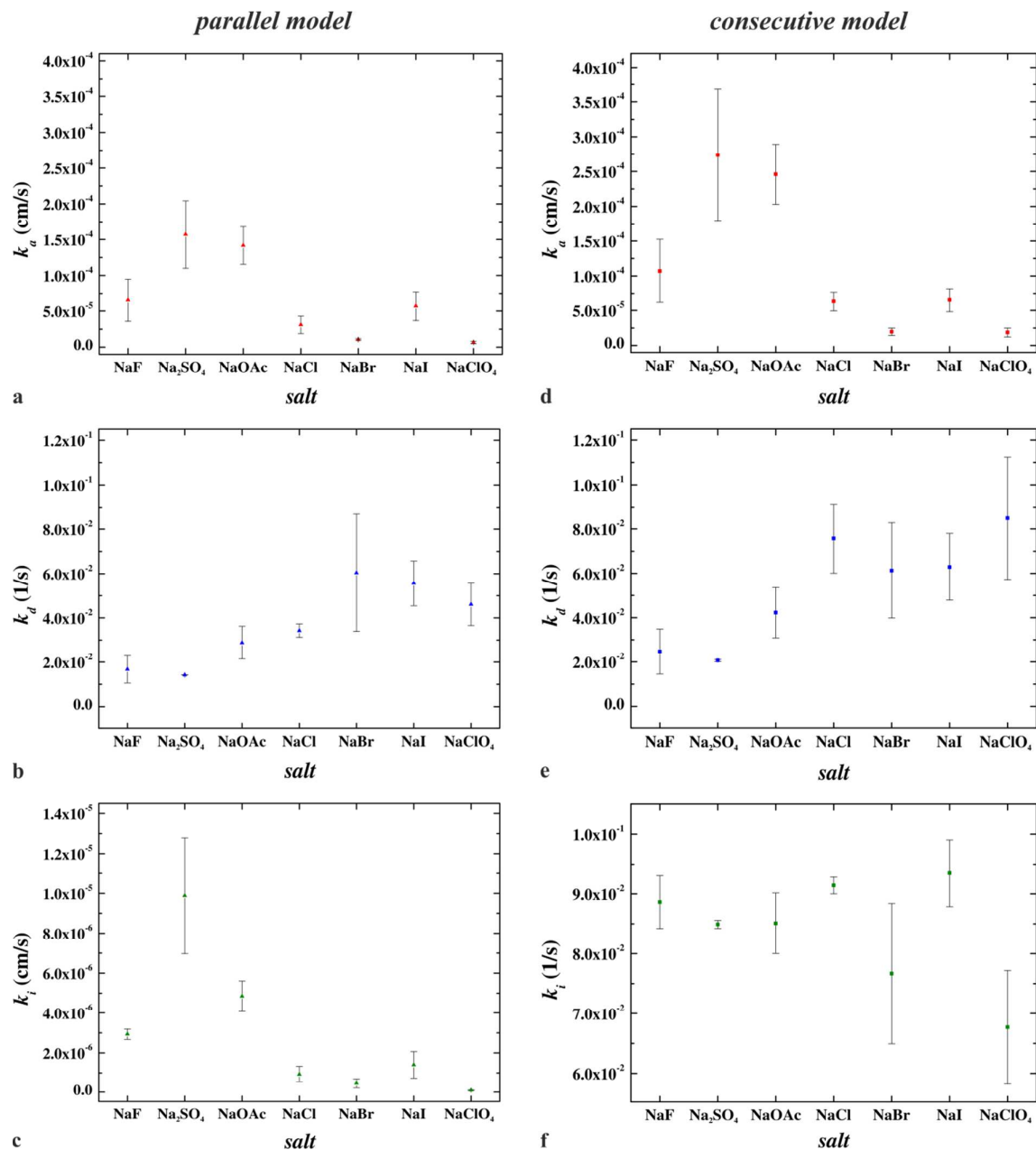


Figure 4 Adsorption-desorption kinetics of flagellin in extreme kosmotropic (NaF) and chaotropic (NaClO_4) solutions evaluated using the parallel model. (a) Calculated concentration profile of the bulk (c_{bulk}) and the diffusion boundary layer (c_v) in the presence of NaClO_4 salt. Flagellin adsorption curves (*orange* - measured, *black* - fitted, *green* - reversibly, *cyan* - irreversibly adsorbed surface mass density) in the presence (b) of the kosmotropic NaF and (c) of the chaotropic NaClO_4 . The numbers on the top of the panels indicate the following experimental phases: **1**: starting buffer for recording the baseline; **2**: administering flagellin solution; **3**: washing with buffer.

All kinetic parameters obtained using both the parallel and the consecutive model are shown in **Fig. 5** and summarized in **Table S1** (see in Supplementary Document).

In case of the parallel model, the k_a and k_i values decrease from kosmotropic to chaotropic salts (**Fig. 5a** and **c**). The k_d values increase from kosmotropes to chaotropes (**Fig. 5b**). The consecutive model demonstrates the same tendency for k_a and k_d values (**Fig. 5d** and **e**). The k_i values do not show a clear tendency (**Fig. 5f**).



1
2
3 **Figure 5** The effect of the Hofmeister series on the reversible adsorption (k_a), the dissociation
4 (k_d), as well as the irreversible adsorption (k_i) rate constants when using (a, b, c) the parallel or
5 (d, e, f) the consecutive model for their calculation.
6
7
8
9
10
11
12
13
14
15
16
17
18
19
20
21
22
23
24
25
26
27
28
29
30
31
32
33
34
35
36
37
38
39
40
41
42
43
44
45
46
47
48
49
50
51
52
53
54
55
56
57
58
59
60

Another parameter of the adsorbed protein is the footprint, which refers to the average area occupied by an adsorbed molecule. The footprints of the reversibly (a_r) and irreversibly (a_i) adsorbed flagellin molecules are shown in **Fig. 6**. Their numerical values are summarized in **Table S2**. It can be seen that both the reversibly and the irreversibly adsorbed footprint of the flagellin increases from kosmotropes to chaotropes in case of both the parallel and the consecutive models.

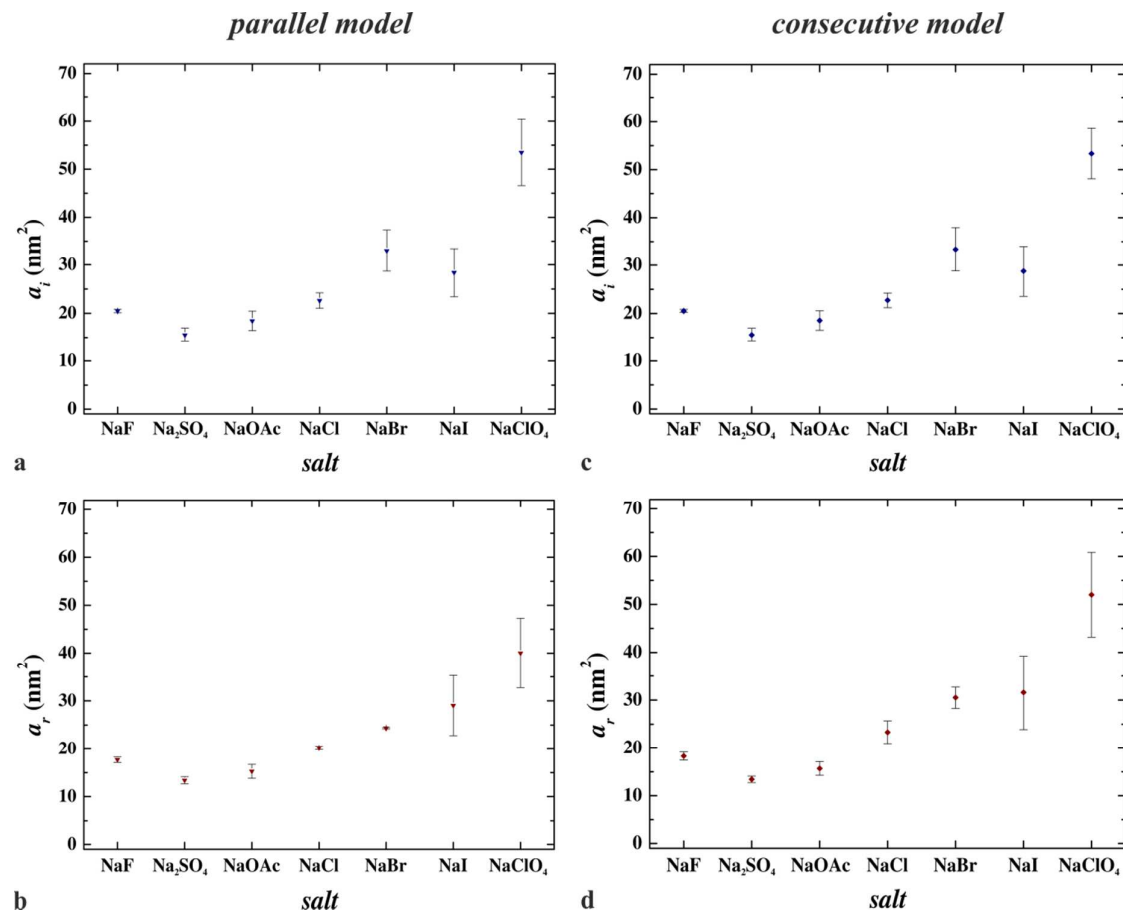


Figure 6 Change of the footprints of reversibly and irreversibly adsorbed flagellin molecules from kosmotropic salts (NaF, Na_2SO_4 , NaOAc) to chaotropic salts (NaBr, NaI, NaClO_4) in case of (a, b) the parallel as well as (c, d) the consecutive model.

3.4. Adsorbed protein layer structure during the adsorption and desorption process

In the following, we investigate in detail the structural changes occurring in the formed protein layer during the adsorption and desorption processes. Our previous work already indicated that flagellin adsorbs on hydrophobic surfaces in an oriented manner, namely, through the disordered terminal regions². However, experiments conducted with a truncated flagellin variant (F40), missing the disordered regions, also revealed a significant surface adsorption, but, with a much slower adsorption rate. This observation indicates that besides the disordered region other parts of the protein can also play a role in the adsorption process. We, therefore concluded that when the disordered region is present, the adsorption is dominant through this part of the protein in the presence of a Hofmeister-neutral salt².

It has to be noted; CD and FTIR experiments suggested that the folded structure of flagellin is only marginally affected by the Hofmeister salts or by adsorption onto hydrophobic surfaces. On the other hand, the previously detailed results revealed, that Hofmeister salts have a strong influence on the adsorption process and both the kinetic rate constants and adsorbed molecular footprints are strongly influenced. These results indicate that most probably the surface orientation, and not the internal structure of the molecule is affected by the Hofmeister salts.

This hypothesis is fully supported by investigating the quasi-homogeneous and isotropic refractive index of the adsorbed molecular layer²⁵ (see **Fig. 7**). The effect of Hofmeister salts can be clearly seen on the variation of refractive index. From kosmotropes to chaotropes the indicated birefringence turns from slightly positive to significantly negative^{2,25,26}. This can be an indication that while in kosmotropic salts the molecules are oriented towards the surface by their terminal regions, in chaotropic salts a laid down arrangement is preferred. The previously obtained molecular footprints and **Fig. 8** strongly support this conclusion.

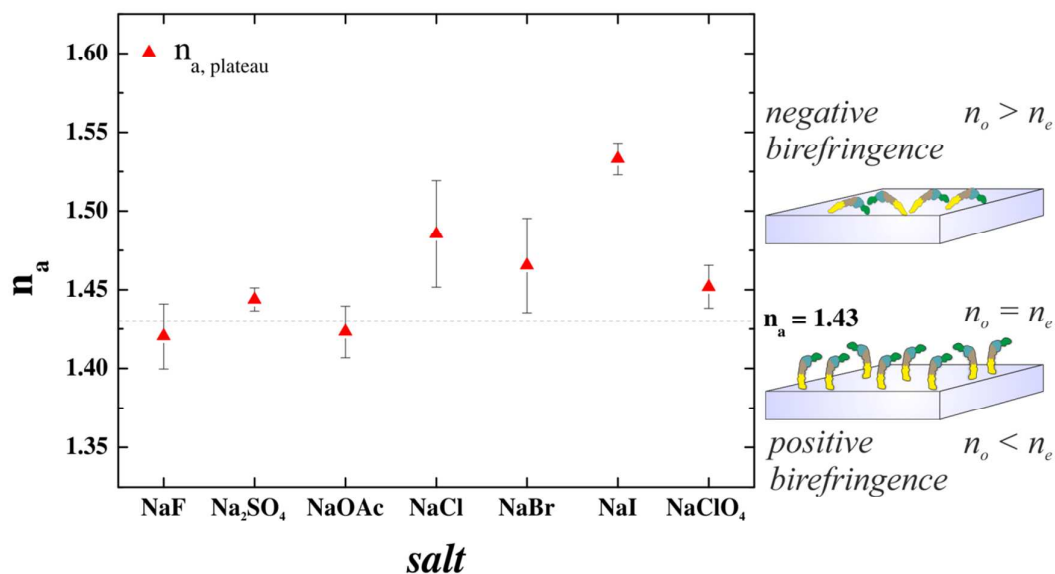


Figure 7 Variation of the refractive index of the flagellin layer along the Hofmeister series. Moving from kosmotropic to chaotropic salts the measured birefringence turns from slightly positive to significantly negative.

In **Fig. 8** the side and top view of the flagellin molecule are shown. The calculated footprint of the top view is approximately 24 nm^2 , while the footprint of the side view is 49 nm^2 , in good agreement with the above results. Note, the footprint values obtained from the kinetic modeling smaller than 24 nm^2 indicate a very densely packed layer, and can be attributed to the slight tilt of the surface showed in **Fig. 8b** with respect to the surface of the biosensor.

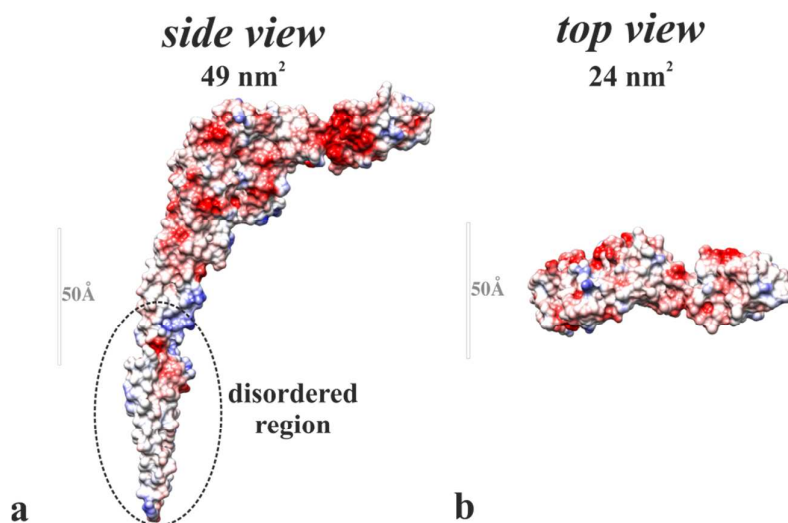


Figure 8 Side (a) and top view (b) of the flagellin molecule. The surface of the protein is colored according to the local charge, from *red* (-) to *blue* (+) scale. The parts close to the *white* show the hydrophobic regions. The footprint of the top view is approximately 24 nm^2 , while the footprint of the side view is 49 nm^2 .

The results of the above findings are summarized in **Fig. 9**, where the preferred molecular orientations in the various adsorbed states are shown. In short, the salts are mainly influence the preferred adsorption surface in the various molecular states. In case of kosmotropic salts, flagellin adsorbs through its disordered terminal regions via hydrophobic interaction and an oriented adsorbed layer is obtained. Lateral hydrophobic interactions between the D1 domains of the subunits, as observed in the filament, might also play a role in the stabilization of the oriented layer. (**Fig. 9** upper inset). But, in chaotropic salts the hydrophobic interaction is weakened and the laid down molecular orientation becomes dominant. Flagellin molecules lie on the longitudinal axis on the surface resulting in a significantly larger adsorbed footprint (see **Fig. 9** bottom inset).

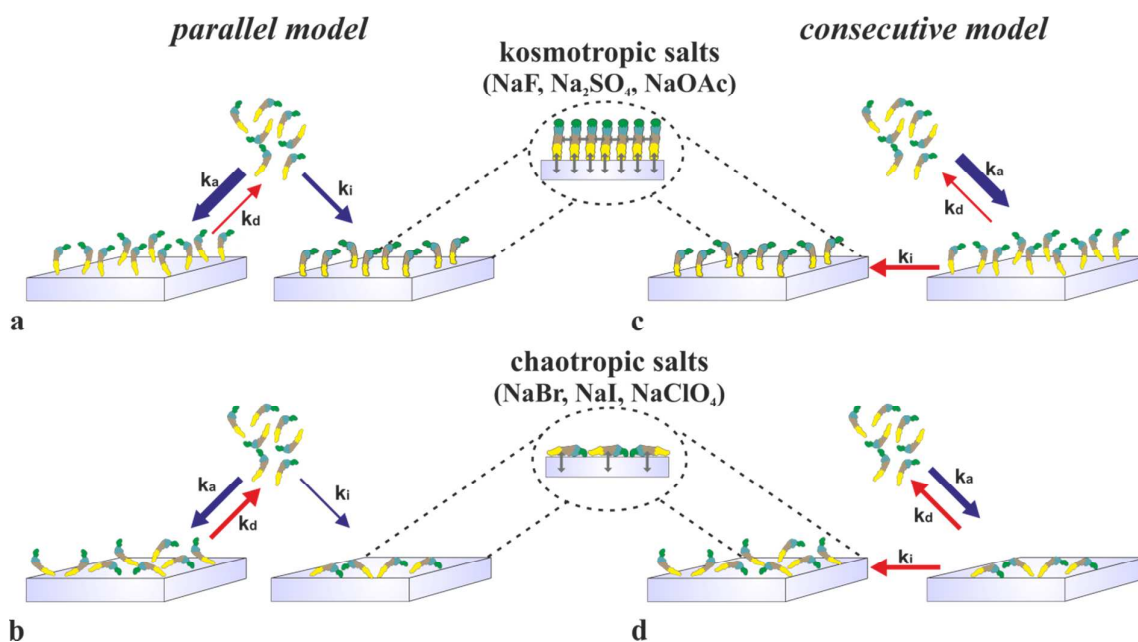


Figure 9 Schematic illustration of the adsorption kinetics of flagellin proteins on a hydrophobic surface (regarding the dimensions, the *blue arrow* refers to cm/s, while the *red arrow* to 1/s, respectively). (a) The kosmotropes (Na₂SO₄, NaF, NaOAc) increase the irreversible adsorption of the flagellin. The footprint of the protein suggests that the flagellin D0 domain interacts with the hydrophobic surface. (b) The chaotropes (NaBr, NaI, NaClO₄) increase the dissociation of the flagellin. The footprint of the protein suggests that the flagellin lies along its longitudinal axis on the surface.

Upper inset shows the supposed interactions between the flagellin and the surface, and the interactions between the proteins. Bottom inset represents the interactions between the laid down flagellins and the surface.

3.5 A simple model to determine the protein-water-substrate interfacial tension in the presence of Hofmeister salts

The above results can be used to estimate the protein-water-substrate interfacial tension (γ_{pws}) of the flagellin protein related to the adsorption process, and its dependence on the Hofmeister salts. We define this new type of surface tension as the specific work of adhesion/adsorption during the protein adsorption process as follows.

One can write for the work of adsorption (Gibbs free energy change characterizing the adsorption process)

$$\Delta G_{\text{ads}} = \Delta G_{\text{pw}} + \Delta G_{\text{sw}} + \Delta G_{\text{ps}}, \quad (11)$$

where ΔG_{pw} , ΔG_{sw} and ΔG_{ps} are the free energy changes at the protein-water (protein-solvent), substrate-water (substrate-solvent) and protein-substrate interfaces. Supposing that a surface adsorbed protein has an area A_{ads} in contact with the substrate and this area was fully exposed to the solvent in the dissolved state before adsorption (Therefore, A_{ads} area is disappearing at the protein-water and substrate-water interfaces, and A_{ads} area is appearing at the protein-substrate interface upon the protein adsorption process), one can write

$$\Delta G_{\text{ads}} = -\gamma_{\text{pw}}A_{\text{ads}} - \gamma_{\text{sw}}A_{\text{ads}} + \gamma_{\text{ps}}A_{\text{ads}}, \quad (12)$$

where γ_{pw} , γ_{sw} and γ_{ps} are the protein-water, substrate-water and protein-substrate interfacial surface tensions, respectively. Therefore, eq. 12 can be written as

$$\Delta G_{\text{ads}} = -(\gamma_{\text{pw}} + \gamma_{\text{sw}} - \gamma_{\text{ps}}) A_{\text{ads}} = -\gamma_{\text{pws}} A_{\text{ads}} \quad (13)$$

where γ_{pws} is the introduced protein-water-substrate surface tension ($\gamma_{\text{pws}} = (\gamma_{\text{pw}} + \gamma_{\text{sw}} - \gamma_{\text{ps}})$).

The adsorption and desorption are thermally activated processes and one can write the following equation

$$\frac{k_a}{k_d \cdot d} = e^{-\frac{\Delta G_{\text{ads}}}{k_B \cdot T}} \quad (14)$$

where k_B is the Boltzmann constant, T is the absolute temperature. Note, the appearance of the d factor, characterizing the thickness of the surface layer, is due to the conversion of k_a with dimensions of cm/s to k_a' with dimension of 1/s. (This simple term converts the volume concentration to surface concentration in a straightforward manner and must be introduced due to the different dimensions of k_a and k_d . Simply, proteins closer to the substrate surface

1
2
3 than d are considered to be surface adsorbed. For example, according to this conversion the
4 adsorption term in Eq. 2 is modified to $k'_a \cdot [c_v \cdot d_p] \cdot \Phi$, with $k'_a = \frac{k_a}{d}$.)

5
6 Therefore, after rearrangement one obtains

$$\Delta G_{\text{ads}} = -k_B \cdot T \cdot \ln \frac{k_a}{k_d \cdot d} \quad (15)$$

7
8
9
10
11 $d = 10$ nm was employed in the numerical calculations, which value is a reasonable
12 approximation of the thickness of the surface adsorbed protein layer. (Note, the calculations
13 were also performed with two additional values (5 nm and 20 nm), which resulted only in
14 slight differences in the ΔG_{ads} values.)

15
16 From Eq. 15 one obtains the following equation for γ_{pws} by using its above definition

17
18 ($\Delta G_{\text{ads}} = -\gamma_{\text{pws}} \cdot A_{\text{ads}}$):

$$\gamma_{\text{pws}} = \frac{k_B \cdot T}{A_{\text{ads}}} \cdot \ln \frac{k_a}{k_d \cdot d} \quad (13)$$

19
20
21
22
23
24
25 where A_{ads} is the adsorption surface area, supposed to be equal to a_r in further calculations.

26
27 **Fig. 10** shows the dependence of ΔG_{ads} and γ_{pws} on the employed Hofmeister salts.
28
29
30
31
32
33
34
35
36
37
38
39
40
41
42
43
44
45
46
47
48
49
50
51
52
53
54
55
56
57
58
59
60

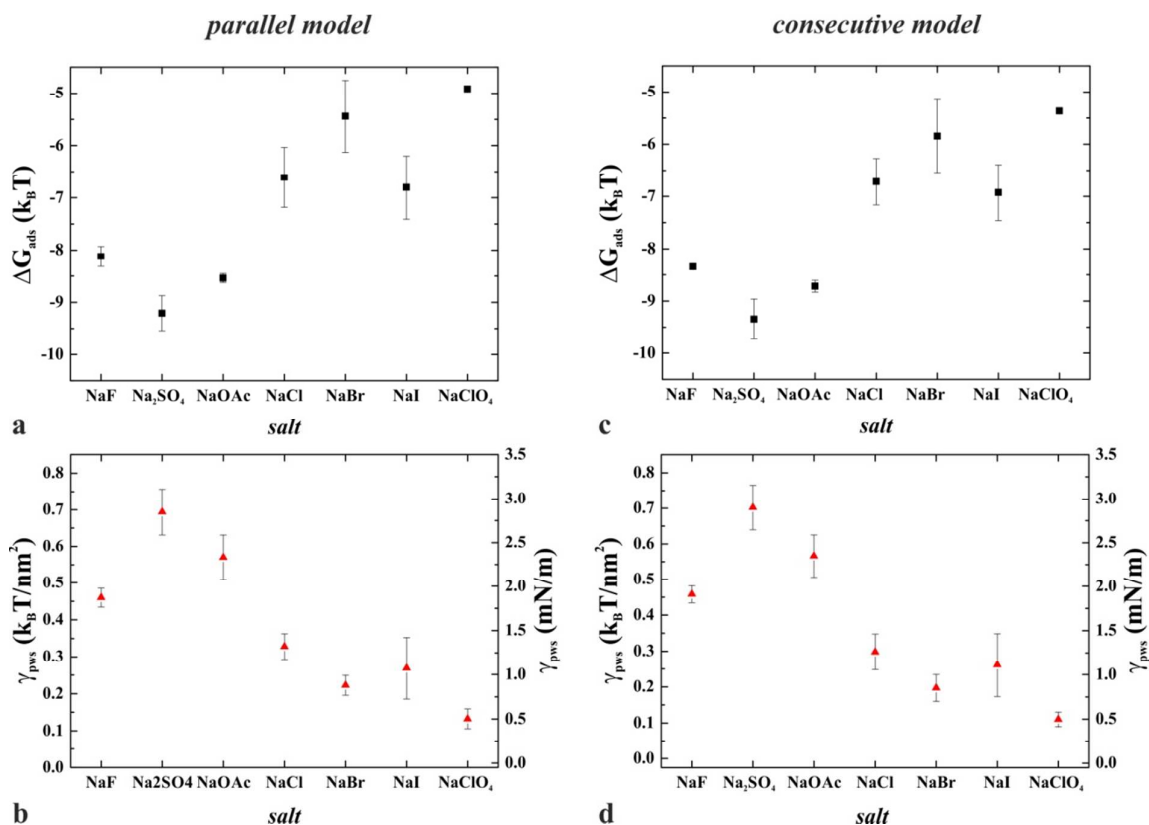


Figure 10 (a, c) Calculated Gibbs free energy difference of the adsorbed and desorbed states and (b, d) protein-water-substrate interfacial tension in the presence of Hofmeister salts supposing parallel and consecutive kinetic models to analyze the OWLS data.

It is apparent that, within the error, both models yielded the same results for the interfacial tension values that essentially follow the Hofmeister series. The only outlier, fluoride slightly deviates from the expected trend, which might be attributed to specific interactions with the protein surface. In general, it can be established that the salt-dependence of all the essential measured quantities (adsorbed mass, kinetic constants, footprints, etc.) follows the tendency of the interfacial tension plots: kosmotropic salts increase γ_{pws} that accompanies with higher adsorbed mass and order parameter, while chaotropic salts exert opposite effects. These observations, together with the model-independence of γ_{pws} values, suggest that, similarly to the role of protein-water interfacial tension in the interpretation of conformation-related phenomena, protein-water-substrate interfacial tension can be considered as a central parameter in the phenomenological description of protein adsorption processes.

1
2
3 To our knowledge, this is the first time when explicit, quantitative experimental data are
4 shown for the absolute value of a protein interfacial tension, namely the protein-water-
5 substrate interfacial tension. Note that, this quantity depends on the water-exposed protein
6 surface (i.e., the hydrophobic/hydrophilic nature of the amino acids at the interface), the
7 nature of the substrate, and the quality and quantity of dissolved cosolutes, as well. In spite of
8 the technical and conceptual difficulties in determining interfacial tension under microscopic
9 conditions¹³, protein-water interfacial tension is considered a key parameter to describe
10 Hofmeister effects and hydrophobic interactions at protein surfaces, in general¹⁴. A higher
11 value implies tighter protein conformation, and increased susceptibility to aggregation and
12 adsorption to hydrophobic surfaces. The latter process, however, is more complex, because
13 the hydrophilic/hydrophobic properties of the substrate should also be taken into account;
14 hence, it is characterized more precisely with the protein-water-substrate interfacial tension
15 (γ_{pws}). As for the related quantity, the protein-water interfacial tension (γ_{pw}), only relative
16 values have been published so far, obtained either from numerical simulations of the Trp-cage
17 miniprotein²¹ or from cloud-point measurements on lysozyme³⁸. Both studies revealed molar
18 salt-induced changes of the protein-water interfacial tension in the order of a few mN/m, in
19 concert with the order and tendency of our data. Note that theoretical and experimental studies
20 of Hofmeister effects at various macroscopic surfaces also established "interfacial tension
21 increment" values consistent with our results^{39,40}, respectively.
22
23
24
25
26
27
28
29
30
31
32
33
34
35
36
37
38
39
40
41
42
43
44
45
46
47
48
49
50
51
52
53
54
55
56
57
58
59
60

5. Conclusions

In this work we studied the effect of Hofmeister salts on the structure and surface adsorption kinetics of wild-type flagellin. Based on our OWLS measurements the kosmotropic Na_2SO_4 , NaF and NaOAc salts and the chaotropic NaI, NaClO_4 and NaBr salts have different effect on the surface mass densities compared to the Hofmeister-neutral NaCl. The kosmotropes increased the surface mass densities in contrast to the chaotropes, which decreased them.

CD and FTIR experiments revealed the effect of Hofmeister salts on the structure of flagellin in solution and the conformational changes upon adsorption onto hydrophobic surfaces. We investigated the effect of the highly kosmotropic and chaotropic NaF and NaClO_4 . The results show that the applied salts do not significantly influence the secondary structure of flagellin in solution.

To determine the kinetic parameters of protein adsorption and desorption we used a home-developed MATLAB code fitting protein adsorption models previously developed by Ramsden³¹⁻³³. The employed parallel and consecutive models showed the same type of behavior for the k_a and k_d values. Considering the k_i values, the parallel model demonstrated a decrease when moving from kosmotropic to chaotropic salts, while the consecutive model did not show a clear tendency. The adsorbed protein footprint of the individual flagellin molecules were also determined by the kinetic modeling. We obtained that the reversibly and the irreversibly adsorbed footprint of the flagellin increases when moving from kosmotropes to chaotropes.

CD and FTIR experiments showed that the salts do not influence the protein structure in solution and on the surface. In contrast, our data show that the salts have a strong influence on the adsorbed mass, the kinetic rate constants and the adsorbed molecular footprints. These results suggest that most probably the surface orientation, and not the internal structure of the molecule is affected by the Hofmeister salts. We analyzed the quasi-homogeneous and isotropic refractive index of the adsorbed molecular layer and the results obtained supported this hypothesis. From kosmotropes to chaotropes the indicated birefringence turns from slightly positive to significantly negative. We concluded that in case of the kosmotropic salts the molecules are oriented towards the surface by their terminal regions, while in chaotropic salts the protein lie down on the surface with a significantly increased adsorption molecular footprint; the salts influence the preferred adsorption surface of the protein. Therefore, the Hofmeister salts influence protein orientation and the structure of the adsorbed layer.

1
2
3 The experimentally obtained kinetic parameters and molecular footprints gave the unique
4 possibility to build a simple model to calculate the protein-water-substrate interfacial surface
5 tension at the nanometer scale in the presence of various Hofmeister salts. The calculated
6 values are consistent with previously published data of surface tension increments, and - to
7 the best of our knowledge - represent the first experimental results for this quantity.
8
9
10
11
12
13
14
15
16
17
18
19
20
21
22
23
24
25
26
27
28
29
30
31
32
33
34
35
36
37
38
39
40
41
42
43
44
45
46
47
48
49
50
51
52
53
54
55
56
57
58
59
60

Acknowledgements

This work was supported by the Momentum Program of the Hungarian Academy of Sciences, the ERC_HU and KH_17 projects of NKFIH, the BIONANO_GINOP-2.3.2-15-2016-00017 project and the OTKA grant NN117849. We thank Noemi Kovacs for her work in the development of the MATLAB code used in initial investigations. Robert Horvath gratefully thanks Prof. Jeremy Ramsden for fruitful discussions about protein adsorption kinetics and for his encouragement to work on the present topic.

Supporting Information Available: Kinetic parameters calculated with the parallel and consecutive models. Footprints of the reversibly and irreversibly adsorbed flagellin molecules. Table S1: kinetic parameters calculated with the parallel and consecutive models
Table S2: footprints of the reversibly and irreversibly adsorbed flagellin

This material is available free of charge via the Internet at <http://pubs.acs.org>.

Author Contributions

RH and AD laid down the ideas behind the present work. BKo performed the OWLS experiments with the help of AB and SK. SK developed the surface hydrophobization protocol. The MATLAB code employed for data analysis was developed by RH and AS. Protein production and CD measurements were performed by BKa, FV. BSz conducted FTIR experiments, analyzed the data and wrote related text. AD supplied the salt solutions. The model to calculate the interfacial surface tension was developed by RH. BKo, AS, AD, FV and RH analyzed the data. BKo made the figures. BKo, AS, AD, FV and RH wrote the paper.

References

- (1) Yonekura, K.; Maki-Yonekura, S.; Namba, K. Complete Atomic Model of the Bacterial Flagellar Filament by Electron Cryomicroscopy. *Nature* **2003**, *424* (6949), 643.
- (2) Kovacs, N.; Patko, D.; Orgovan, N.; Kurunczi, S.; Ramsden, J. J.; Vonderviszt, F.; Horvath, R. Optical Anisotropy of Flagellin Layers: In Situ and Label-Free Measurement of Adsorbed Protein Orientation Using OWLS. *Anal. Chem.* **2013**, *85* (11), 5382.
- (3) Kovacs, B.; Patko, D.; Szekacs, I.; Orgovan, N.; Kurunczi, S.; Sulyok, A.; Khanh, N. Q.; Toth, B.; Vonderviszt, F.; Horvath, R. Flagellin Based Biomimetic Coatings: From Cell-Repellent Surfaces to Highly Adhesive Coatings. *Acta Biomater.* **2016**, *42*, 66.
- (4) Kovacs, B.; Patko, D.; Klein, A.; Kakasi, B.; Saftics, A.; Kurunczi, S.; Vonderviszt, F.; Horvath, R. Bacteria Repellent Layer Made of Flagellin. *Sensors Actuators B Chem.* **2018**, *257*, 839.
- (5) Bereczk-Tompa, É.; Vonderviszt, F.; Horváth, B.; Szalai, I.; Pósfai, M. Biotemplated Synthesis of Magnetic Filaments. *Nanoscale* **2017**, 15062.
- (6) Bereczk-Tompa, É.; Pósfai, M.; Tóth, B.; Vonderviszt, F. Magnetite-Binding Flagellar Filaments Displaying the MamI Loop Motif. *ChemBioChem* **2016**, *17* (21), 2075.
- (7) Klein, Á.; Kovács, M.; Muskotál, A.; Jankovics, H.; Tóth, B.; Pósfai, M.; Vonderviszt, F. Nanobody-Displaying Flagellar Nanotubes. *Sci. Rep.* **2018**, *8* (1), 3584.
- (8) Tanford, C. Interfacial Free Energy and the Hydrophobic Effect. *Proc. Natl. Acad. Sci. U. S. A.* **1979**, *76* (9), 4175.
- (9) Chothia, C.; Janin, J. Principles of Protein–protein Recognition. *Nature* **1975**, *256* (5520), 705.
- (10) Record, M. T.; Guinn, E.; Pegram, L.; Capp, M. Introductory Lecture: Interpreting and Predicting Hofmeister Salt Ion and Solute Effects on Biopolymer and Model Processes Using the Solute Partitioning Model. *Faraday Discuss.* **2013**, *160*, 9.
- (11) Lo Nostro, P.; Ninham, B. W. Hofmeister Phenomena: An Update on Ion Specificity in Biology. *Chem. Rev.* **2012**, *112* (4), 2286.
- (12) Okur, H. I.; Hladílková, J.; Rembert, K. B.; Cho, Y.; Heyda, J.; Dzubiella, J.; Cremer, P. S.; Jungwirth, P. Beyond the Hofmeister Series: Ion-Specific Effects on Proteins and Their Biological Functions. *J. Phys. Chem. B* **2017**, *121* (9), 1997.
- (13) Dér, A.; Kelemen, L.; Fábrián, L.; Taneva, S. G.; Fodor, E.; Páli, T.; Cupane, A.; Cacace, M. G.; Ramsden, J. J. Interfacial Water Structure Controls Protein Conformation. *J. Phys. Chem. B* **2007**, *111* (19), 5344.
- (14) Násztor, Z.; Bogár, F.; Dér, A. The Interfacial Tension Concept, as Revealed by Fluctuations. *Curr. Opin. Colloid Interface Sci.* **2016**, *23*, 29.
- (15) Collins, K. D.; Washabaugh, M. W. The Hofmeister Effect and the Behavior of Water at Interfaces. *Q. Rev. Biophys.* **1985**, *18* (4), 323.

- 1
2
3 (16) Cacace, M. G.; Landau, E. M.; Ramsden, J. J. The Hofmeister Series: Salt and Solvent
4 Effects on Interfacial Phenomena. *Q. Rev. Biophys.* **1997**, *30* (3), 241.
- 5
6 (17) Khoroshyy, P.; Dér, A.; Zimányi, L. Effect of Hofmeister Cosolutes on the Photocycle
7 of Photoactive Yellow Protein at Moderately Alkaline PH. *J. Photochem. Photobiol. B*
8 *Biol.* **2013**, *120*, 111.
- 9
10 (18) Szalontai, B.; Nagy, G.; Krumova, S.; Fodor, E.; Páli, T.; Taneva, S. G.; Garab, G.;
11 Peters, J.; Dér, A. Hofmeister Ions Control Protein Dynamics. *Biochim. Biophys. Acta*
12 **2013**, *1830* (10), 4564.
- 13
14 (19) Neagu, A.; Neagu, M.; Dér, A. Fluctuations and the Hofmeister Effect. *Biophys. J.*
15 **2001**, *81* (3), 1285.
- 16
17 (20) Dér, A.; Ramsden, J. J. Evidence for Loosening of a Protein Mechanism.
18 *Naturwissenschaften* **1998**, *85*, 353.
- 19
20 (21) Bogár, F.; Bartha, F.; Násztor, Z.; Fábián, L.; Leitgeb, B.; Dér, A. On the Hofmeister
21 Effect: Fluctuations at the Protein-Water Interface and the Surface Tension. *J. Phys.*
22 *Chem. B* **2014**, *118* (29), 8496.
- 23
24 (22) Nelson, N.; Schwartz, D. K. Specific Ion (Hofmeister) Effects on Adsorption,
25 Desorption, and Diffusion at the Solid-Aqueous Interface. *J. Phys. Chem. Lett.* **2013**, *4*
26 (23), 4064.
- 27
28 (23) Salis, A.; Medda, L.; Cugia, F.; Monduzzi, M. Effect of Electrolytes on Proteins
29 Physisorption on Ordered Mesoporous Silica Materials. *Colloids Surfaces B*
30 *Biointerfaces* **2016**, *137*, 77.
- 31
32 (24) Orgovan, N.; Patko, D.; Hos, C.; Kurunczi, S.; Szabó, B.; Ramsden, J. J.; Horvath, R.
33 Sample Handling in Surface Sensitive Chemical and Biological Sensing: A Practical
34 Review of Basic Fluidics and Analyte Transport. *Adv. Colloid Interface Sci.* **2014**, *1*.
- 35
36 (25) Horvath, R.; Ramsden, J. J. Quasi-Isotropic Analysis of Anisotropic Thin Films on
37 Optical Waveguides. *Langmuir* **2007**, *23* (18), 9330.
- 38
39 (26) Horvath, R.; Kobzi, B.; Keul, H.; Moeller, M.; Kiss, É. Molecular Interaction of a New
40 Antibacterial Polymer with a Supported Lipid Bilayer Measured by an in Situ Label-
41 Free Optical Technique. *Int. J. Mol. Sci.* **2013**, *14* (5), 9722.
- 42
43 (27) Stalder, A. F.; Kulik, G.; Sage, D.; Barbieri, L.; Hoffmann, P. A Snake-Based
44 Approach to Accurate Determination of Both Contact Points and Contact Angles.
45 *Colloids Surfaces A Physicochem. Eng. Asp.* **2006**, *286* (1–3), 92.
- 46
47 (28) Vonderviszt, F.; Kanto, S.; Aizawa, S.; Namba, K. Terminal Regions of Flagellin Are
48 Disordered in Solution. *J. Mol. Biol.* **1989**, *209* (1), 127.
- 49
50 (29) Tiefenthaler, K.; Lukosz, W. Sensitivity of Grating Couplers as Integrated-Optical
51 Chemical Sensors. *J. Opt. Soc. Am. B* **1989**, *6* (2), 209.
- 52
53 (30) De Feijter, J.; Benjamins, J.; Veer, F. Ellipsometry as a Tool to Study the Adsorption
54 Behavior of Syntetic and Biopolymers at the Air Water Interface. *Biopolymers* **1978**, *17*
55 (7), 1759.
- 56
57
58
59
60

- 1
2
3 (31) Kurrat, R.; Prenosil, J. E.; Ramsden, J. J. Kinetics of Human and Bovine Serum
4 Albumin Adsorption at Silica-Titania Surfaces. *J. Colloid Interface Sci.* **1997**, *185* (1),
5 1.
6
7 (32) Ansari, F.; Kavosh, M.; Horvath, R.; Ghalamboran, M. R.; Ramsden, J. J. Bacterial
8 Adsorption onto Monolayer Ferromagnetic Nanofilms. *J. Bionanoscience* **2010**, *4* (1–
9 2), 119.
10
11 (33) Ansari, F.; Kavosh, M.; Horvath, R.; Ramsden, J. J. Particle Speciation during PEG-
12 Fe₃O₄ Hybrid Nanoparticle Self-Assembly on Si(Ti)O₂. *J. Nanoparticle Res.* **2011**, *13*
13 (1), 193.
14
15 (34) Viot, P.; Tarjus, G.; Ricci, S. M.; Talbot, J. Random Sequential Adsorption of
16 Anisotropic Particles. I. Jamming Limit and Asymptotic Behavior. *J. Chem. Phys.*
17 **1992**, *97* (7), 5212.
18
19 (35) Malmsten, M. *Biopolymers at Interfaces, Second Edition*; 2003.
20
21 (36) Vonderviszt, F.; Uedaira, H.; Kidokoro, S. I.; Namba, K. Structural Organization of
22 Flagellin. *J. Mol. Biol.* **1990**, *214* (1), 97.
23
24 (37) Pelton, J. T.; McLean, L. R. Spectroscopic Methods for Analysis of Protein Secondary
25 Structure. *Anal. Biochem.* **2000**, *277* (2), 167.
26
27 (38) Zhang, Y.; Cremer, P. S. The Inverse and Direct Hofmeister Series for Lysozyme.
28 *Proc. Natl. Acad. Sci. U. S. A.* **2009**, *106* (36), 15249.
29
30 (39) dos Santos, A. P.; Levin, Y. Surface and Interfacial Tensions of Hofmeister
31 Electrolytes. *Faraday Discuss.* **2013**, *160* (June 2013), 75.
32
33 (40) Melander, W.; Horváth, C. Salt Effects on Hydrophobic Interactions in Precipitation
34 and Chromatography of Proteins: An Interpretation of the Lyotropic Series. *Arch.*
35 *Biochem. Biophys.* **1977**, *183* (1), 200.
36
37
38
39
40
41
42
43
44
45
46
47
48
49
50
51
52
53
54
55
56
57
58
59
60

1
2
3
4
5
6
7
8
9
10
11
12
13
14
15
16
17
18
19
20
21
22
23
24
25
26
27
28
29
30
31
32
33
34
35
36
37
38
39
40
41
42
43
44
45
46
47
48
49
50
51
52
53
54
55
56
57
58
59
60

TOC Graphic

